Environmental Science & Technology

pubs.acs.org/est

Article

Impacts of Removal Compensation Effect on the Mercury Emission Inventories for Nonferrous Metal (Zinc, Lead, and Copper) Smelting in China

Shuzhen Cao, Lei Zhang,* Yang Zhang, Shuxiao Wang, and Qingru Wu

Cite This: *Environ. Sci. Technol.* 2022, 56, 2163−2171

Read Online

ACCESS | Metrics & More | Article Recommendations | Supporting Information

Downloaded via NANJING UNIV on February 15, 2022 at 09:47:14 (UTC).
See https://pubs.acs.org/sharingguidelines for options on how to legitimately share published articles.

ABSTRACT: Nonferrous metal smelting (NFMS) is one of the key sources of mercury (Hg) emissions to the air and cross-media Hg transfer in China. In this study, a "Hg removal compensation effect" between upstream and downstream air pollution control devices (APCDs) in NFMS was uncovered based on the investigation of field test data. The relationships between the Hg concentration in flue gas and the Hg removal efficiencies of typical APCDs were established, and an advanced probabilistic mass flow model regarding this effect was developed. Model comparison shows that the probabilistic essence of the advanced model prevents the underestimation of the deterministic model caused by using the geometric means of the Hg contents of metal concentrates, and the consideration of the removal compensation effect leads to more accurate estimation of the overall Hg removal efficiency of cascaded APCDs. The Hg emission abatement in the NFMS sector from 2010 to 2017 was evaluated to be 55.6 t, which was 13.5% higher than the estimate without considering the Hg removal compensation effect. The overall uncertainty of the improved model was reduced. This study provides a new methodology for more accurate evaluation of the effectiveness of the national implementation plan for the Minamata Convention on Mercury.

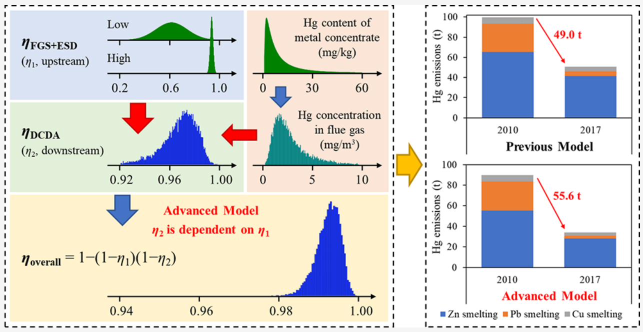

KEYWORDS: *Hg emission inventory, nonferrous metal smelting, China, Minamata Convention, air pollution control devices, effectiveness*

1. INTRODUCTION

Mercury (Hg) is a global pollutant due to its toxicity, persistence, long-distance transport, and bioaccumulation.[1,2] To reduce global Hg emissions and releases, the Minamata Convention on Mercury was signed by 128 countries in 2013 and entered into force in 2017.[3] China is the largest anthropogenic Hg emitter in the world.[4−7] Nonferrous metal smelting (NFMS), as one of the five key Hg emission sources addressed in the Minamata Convention, is one of the most important emission sectors in China.[3,8] NFMS herein refers to zinc (Zn), lead (Pb), and copper (Cu) smelting. Based on the estimation of Zhang et al.,[9] the annual Hg emission from the NFMS sector in China was in the range of 96.4−146.4 t during the period of 2000−2010 and accounted for 18 to 33% of the total anthropogenic Hg emissions in China, next only to coal combustion. Liu et al.[10] estimated the NFMS Hg emissions in China in 2017 to be 68 t, accounting for 15% of the total anthropogenic Hg emissions in China.

Studies on Hg emission inventories for the NFMS sector in China date back to the early 2000s. Pacyna et al.[6,11,12] used emission factors from the United Nations Economic Commission for Europe database[13] in the calculation of atmospheric Hg emission from the Chinese NFMS sector when developing the global inventories of anthropogenic Hg emissions in 1995, 2000, and 2005, respectively. Streets et al.[4] and Wu et al.[14] brought the inventory to the provincial level for China using the provincial emission factor data from Jiang et al.[15] and Feng et al.[16] for Zn smelting and estimated the NFMS Hg emissions (excluding those from gold smelting) to be 134.5−275.9 t from 1995 to 2003. Without considering the cobenefiting Hg removal efficiencies of air pollution control devices (APCDs), these figures were prone to be overestimated. Hylander and Herbert[17] estimated China's Hg emissions from NFMS in 2005 to be 83 t with the cobenefiting Hg removal of acid plants in the smelters considered, and the estimate was brought down significantly. Wu et al.[18] adopted a technology-based method using the geometric means of Hg contents of metal concentrates by province and updated the Hg emission inventories for NFMS in China during 2000−2010, yielding an annual emission range of 67.6−100.1 t. The

Received: August 17, 2021
Revised: January 13, 2022
Accepted: January 14, 2022
Published: January 25, 2022

ACS Publications

© 2022 American Chemical Society

https://doi.org/10.1021/acs.est.1c05523
Environ. Sci. Technol. 2022, 56, 2163−2171

databases of Hg contents of metal concentrates and Hg removal efficiencies of APCDs were updated based on new results from sample analyses and field measurements. In addition to the technology-based methodology, Zhang et al.[9] introduced the Monte Carlo simulation into the inventory model, considering the probability distributions of key input parameters, and found the Hg emission estimates to be 40–50% higher than those from Wu et al.[18] Wu et al.[19] inherited this methodology and estimated the temporal trend of atmospheric Hg emissions in China from 1978 to 2014 and found 116 t of Hg emitted from the NFMS sector in 2014. Wu et al.[20] used the mass flow model with the Monte Carlo technique to quantify Hg output to different environmental media in the NFMS sector and obtained an estimate of 100.4 t Hg emitted into the air in 2012.

The improvement of the methodology in Hg emission estimation for the NFMS sector in China experienced three steps: (1) the uniform emission factor method was replaced by the technology-based method based on new concentrate Hg content data from sample analyses,[18,21] and localized APCD Hg removal efficiency data from field measurements;[22–24] (2) the Monte Carlo simulation was introduced into the method turning deterministic model into probabilistic model, in which the probability distributions of key parameters were considered and the underestimation from the use of geometric mean was avoided;[9,19] (3) the evolution from the emission factor model to the mass flow model shifted the focus from the mainstream roasting/smelting stage to the whole smelting procedure including four stages, resulting in more accurate estimation of Hg emissions from different stacks into the air and the quantification of cross-media Hg transfers.[20,24–27]

The accuracy of the Hg emission inventory for the NFMS sector in China has been greatly improved based on the above three steps. Another step to further reduce the uncertainty of the Hg emission inventory is to take into consideration the relationship between the concentrations of flue gas constituents and the Hg removal efficiency of APCDs. Our previous study[28] linked the Hg removal efficiency of APCDs for coal-fired power plants (CFPPs) to Hg and chlorine (Cl) concentrations in flue gas and found a 6% underestimation of Hg emissions from the CFPP sector in China without considering the dependence of the Hg removal efficiency on Hg and Cl concentrations. The flue gas Cl concentration plays an important role in Hg removal for coal combustion, while the flue gas Hg concentration could have a higher impact in the NFMS sector. On-site measurements[23,29,30] have shown that higher Hg concentration at the inlet usually results in a higher Hg removal efficiency of an APCD. Therefore, when the upstream APCD has a lower Hg removal rate than average, it causes higher Hg concentration at the inlet of the downstream APCD, resulting in a higher Hg removal rate inside the downstream APCD than average. This phenomenon is named the "Hg removal compensation effect" in this study. It describes the dependency between Hg removal efficiencies of two cascaded APCDs. Existing inventory models[9,19,20,25] all assumed the Hg removal efficiencies of different APCDs to be independent. The overlook of the Hg removal compensation effect could cause underestimation of the total Hg removal efficiency, and the impacts will be amplified when more advanced APCDs are adopted in the NFMS sector.

In this study, the Hg removal compensation effect was quantified based on existing field measurements, and an advanced probabilistic mass flow model regarding this effect was developed to estimate Hg emissions from NFMS in China in 2010 and 2017. Comparison of three inventory models was conducted to quantify the impacts of this effect. The effectiveness of Hg emission control measures taken in the NFMS sector in China between 2010 and 2017 was evaluated with and without considering the removal compensation effect. This study has proposed an optimized method in the development of Hg emission inventories for the NFMS sector and could contribute to more accurate evaluation of the effectiveness of the national implementation plans for the Minamata Convention on Mercury.

2. METHODOLOGY

2.1. Mass Flow Model Description. The atmospheric Hg emissions in the NFMS sector originate mainly from metal concentrates (>97%).[24] Hg in raw materials enters flue gases through high-temperature processes and gets removed across APCDs, with the remaining Hg emitted into the atmosphere through exhausted flue gases.[23] As shown in Figure S1 in the Supporting Information, the whole NFMS procedure can be divided into four stages: concentrate dehydration, roasting or smelting, metal extraction, and reclaiming or refining.[23] The mainstream flue gas comes from the roasting/smelting stage, followed successively by the dust collector (DC), flue gas scrubber (FGS), electrostatic demister (ESD), mercury reclaiming tower, if any, acid plant mostly with the double-contact-double-absorption (DCDA) process, and the flue gas desulfurization (FGD) system, if any. Multiple smelting technologies were adopted for Zn, Pb, and Cu smelting. Therefore, technology-based mass flow models were utilized in this study for the development of atmospheric Hg emission inventories for the NFMS sector in China by province. The Hg mass flow methodology was adapted from Wu.[24] Three models based on the methodology were established. Details on the methodology can be found in Section S1 in the Supporting Information. Only the estimation methods in the three models for the atmospheric Hg emission from the roasting/smelting exhausted flue gas are introduced as follows for comparison.

2.1.1. Deterministic Mass Flow Model. The estimation method for the atmospheric Hg emission from the roasting/smelting exhausted flue gas in the deterministic mass flow model (model 1) can be described by the following equation

$$E = \sum_{i} \sum_{j} C_i \cdot M_i \cdot \gamma_j \cdot \sum_{k} \left(P_{jk} \cdot \prod_{l} (1 - \eta_{kl}) \right) \quad (1)$$

where E is the Hg emission from NFMS, t/year; i is the province; j is the smelting technology type; k is the type of APCD combinations; l is the lth APCD in the kth combination; C is the consumption of the metal concentrate, Mt/year; M is the Hg content of the consumed metal concentrate, mg/kg; γ is the Hg release rate at the smelting stage; P_{jk} is the application rate of the kth APCD combination in the jth technology; and η_{kl} is the Hg removal efficiency of the lth APCD in the kth combination.

2.1.2. Probabilistic Mass Flow Model. Parameters such as the Hg content of the concentrate and the Hg removal efficiency of the APCD have skewed probability distribution, which could result in the inaccuracy of the deterministic mass flow model. Therefore, the probabilistic mass flow model (model 2) was developed to take this factor into consideration. The estimation method for the atmospheric Hg emission from

https://doi.org/10.1021/acs.est.1c05523
Environ. Sci. Technol. 2022, 56, 2163–2171

the roasting/smelting exhausted flue gas in model 2 can be described by the following equation

$$E(\{x_i\}, \{y_l\}) = \sum_i \sum_j C_i \cdot M_i(x_i) \cdot \gamma_j \cdot \sum_k \left(P_{jk} \cdot \prod_l (1 - \eta_{kl}(y_l)) \right) \quad (2)$$

where $E(\{x_i\},\{y_l\})$ is the probability distribution of the Hg emission from NFMS; $M_i(x_i)$ is the probability distribution of the Hg content of consumed metal concentrate in the ith province; $\eta_{kl}(y_l)$ is the probability distribution of the Hg removal efficiency of the lth APCD in the kth combination. The subscript l for the random variable y indicates that the Hg removal efficiencies of different APCDs are independent in model 2.

2.1.3. Advanced Probabilistic Mass Flow Model Regarding Flue Gas Hg Concentration. According to eq 2, the Hg removal efficiencies of cascaded APCDs have independent probability distribution in model 2. However, the Hg removal efficiencies of APCDs are actually affected by the inlet flue gas Hg concentration, and hence, the Hg removal efficiencies of cascaded APCDs are dependent. In addition to the probabilistic mass flow model, a submodel was introduced into the advanced probabilistic mass flow model (model 3) to describe the effect of the flue gas Hg concentration on the Hg removal efficiencies of APCDs. The estimation method for the atmospheric Hg emission from the roasting/smelting exhausted flue gas in model 3 can be described by the following equation

$$E(\{x_i\}) = \sum_i \sum_j C_i \cdot M_i(x_i) \cdot \gamma_j \cdot \sum_k \left(P_{jk} \cdot \prod_l (1 - \eta_{kl}(M_i(x_i))) \right) \quad (3)$$

where $E(\{x_i\})$ is the probability distribution of the Hg emission from NFMS; $\eta(M(x))$ is the Hg removal efficiency of APCDs as a function of the Hg concentration in flue gas at the inlet, which is related to the Hg content of the metal concentrate. The relationship between the Hg concentration in flue gas and the Hg removal efficiency of APCDs is quantified by a submodel for model 3 and discussed in detail in Section 2.3.

An emission inventory model named the China atmospheric mercury emission (CAME) model with four levels of methods was developed in our previous study.[9] Based on the availability of essential information, Hg emission sources were ranked into four tiers, and higher levels of methodology were applied to higher tiers of sources. Model 2 and model 3 discussed in this study match tier 3 and tier 4 in the CAME model, respectively. In the original CAME model, NFMS was ranked into tier 3. Therefore, the more advanced model 3 developed in this study regarding the Hg removal compensation effect is a level-up of the methodology for the NFMS sector in China.

2.2. Activity Levels and Key Parameters. *2.2.1. Activity Level Data.* The reference years in this study were selected to be 2010 and 2017. The year 2010 is a benchmark year when more advanced APCDs started to be applied to NFMS, and 2017 is the year when the Minamata Convention on Mercury entered into force and the Action Plan on Prevention and Control of Air Pollution in China was completely implemented. The activity level data of the NFMS sector include the amounts of nonferrous metal production, the application rates of smelting technologies, and the application rates of APCD combinations. Detailed data are listed in Tables S1−S3 in the Supporting Information.[31,32] According to consultation with experts from the Chinese Nonferrous Metal Industry Association, outdated production capacity in the NFMS sector was gradually eliminated from 2010 to 2017, so we further updated the application rates of smelting technologies and APCD combinations on the basis of previous studies,[9,10,18,19,33] which are shown in Tables S4 and S5 in the Supporting Information.

2.2.2. Hg Contents of Metal Concentrates. Based on previous studies,[9,18,21] the data of the Hg contents of metal concentrates as produced by province are summarized as Table S6 in the Supporting Information. To calculate the Hg contents of the concentrates as consumed by province, interprovincial concentrate transport matrices for the three types of metal concentrates were established including concentrate import based on consultation and previous studies.[18] The transport matrices of Zn, Pb, and Cu concentrates used for 2010 and 2017 are given in Tables S7−S12 in the Supporting Information. From 2010 to 2017, the import of Zn concentrates increased significantly, especially to Shaanxi, Yunnan, and Hunan; the transport of Pb concentrates from other provinces to Hunan increased considerably; and the import of Cu concentrates almost doubled. The import of Zn and Cu concentrates could reduce the average level of the Hg content of metal concentrates.

For model 1, the geometric means of the Hg contents of metal concentrates were used, while for model 2 and 3, the Hg contents by province were all assumed to fit lognormal distribution.

2.2.3. Hg Removal Efficiencies of APCDs. The Hg removal efficiency of APCDs is a key parameter for the estimation of atmospheric Hg emissions. Onsite measurement results from existing studies were investigated for the Hg removal efficiencies of APCDs for NFMS.[22−24,30,34] Table S13 shows the mean Hg removal efficiencies of APCDs used in model 1. In model 2, the Hg removal efficiencies of FGS + ESD, DCDA, and FGD were assumed to fit normal distribution. In model 3, the Hg removal efficiencies of the high-efficiency cascaded APCDs were determined using the submodel, which is introduced in Section 2.3.

2.3. Submodel for the Advanced Probabilistic Mass Flow Model. In model 3, a submodel was developed to determine the Hg removal efficiencies of absorption-based APCDs, such as FGS + ESD, DCDA, and FGD, where the relationship between the inlet Hg concentration and the Hg removal efficiency exists. According to expert consultation, there are mainly two types of FGS, including a high-efficiency FGS (e.g., dynamic wave scrubber) and a low-efficiency FGS (e.g., tower scrubber), currently used in nonferrous metal smelters in China. The Hg removal efficiencies of FGS + ESD for the two types of FGS were determined based on limited onsite measurement data in previous studies.[22,23] The arithmetic means of the Hg removal efficiencies for high- and low-efficiency scrubbers were 93 and 63%, respectively. There were not enough data to investigate the relationships between the inlet Hg concentration and the Hg removal efficiency of the FGS + ESD. Therefore, the efficiencies of the FGS + ESD were differentiated only by type in the submodel.

https://doi.org/10.1021/acs.est.1c05523
Environ. Sci. Technol. 2022, 56, 2163−2171

To quantify the relationship between the inlet Hg concentration in flue gas and the Hg removal efficiencies of DCDA and FGD, the results from field tests[22,23,34] in nine smelters were collected (basic information on the smelters as shown in Table S14). For DCDA, the major forms of Hg at the inlet flue gas were Hg^{2+} and Hg^0. Previous studies have shown that Hg^{2+} could be reduced to Hg^0 by SO_3^{2-} in the contact tower of DCDA, and Hg^0 could be oxidized and absorbed by concentrated sulfuric acid in the absorption tower.[24] Hg^{2+} is soluble in water, so DCDA also has a strong removal efficiency on Hg^{2+}. Based on the field test results, it was found that, with the increase of the total Hg concentration at the inlet of DCDA (C_{DCDA}), the Hg removal efficiency of DCDA (η_{DCDA}) increases. To better reflect the features of the relationship and avoid the Hg removal efficiency from exceeding 100%, the inlet total Hg concentration in flue gas was processed into the logarithmic form as $\ln(C_{DCDA})$, and the Hg removal efficiency of DCDA was processed in the form of $\ln(1 - \eta_{DCDA})$. A significant linear correlation was found for the two items, as shown in Figure 1, with goodness of fit $R^2 = 0.63$ ($p = 0.006$).

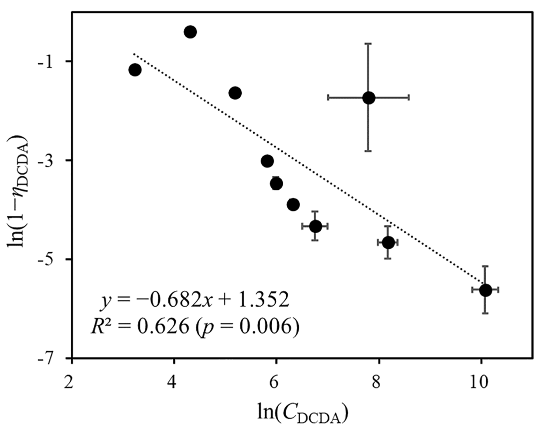

Figure 1. Relationship between the inlet total Hg concentration in flue gas (C_{DCDA}) and the Hg removal efficiency (η_{DCDA}) of DCDA based on field measurements.[22,23,34] Note that the unit of C_{DCDA} is $\mu g/m^3$, and the bidirectional error bars stand for the standard deviations of duplicate samples from field tests that were available.

In addition, the relationship between the inlet Hg concentration in flue gas and the Hg removal efficiency of FGD was also investigated. Due to the inadequacy of data for smelters, field test data from power plants in China were adapted here.[35,36] The Hg in the flue gas removed by FGD was mainly in the form of Hg^{2+}. The inlet concentration of Hg^{2+} and the operational condition of FGD were the two main factors affecting the capture rate of Hg^{2+}. A multiple linear regression was performed with the Hg^{2+} removal efficiency of FGD (η_{FGD}) as the dependent variable and the logarithm of the FGD inlet Hg^{2+} concentration [ln (C_{FGD})] and the FGD desulfurization efficiency (η_{SO2}) as the independent variables (Figure S2). The coefficient of the multivariate linear correlation was 0.94 ($p = 0.001$).

It should be noted that the relationship between inlet Hg concentration and Hg removal efficiency of APCD is not unique for NFMS. In our previous study,[37] the mechanism of this relationship was discussed based on bench-scale experiments and theoretical calculation, and the relationship was put into use in an inventory model via statistical methodology.[28] However, Hg concentration in flue gas is not the only factor that has influence on Hg removal efficiency of APCD. Other factors such as the Cl concentration in flue gas also have significant impacts. The reason why the Hg removal compensation effect was revealed in NFMS flue gas is due to the extremely high Hg concentration level (2−3 orders of magnitude higher than that in the CFPP flue gas).

2.4. Uncertainty Analysis. Monte Carlo simulations were used to analyze the uncertainties of Hg emission estimates. The simulation was performed using Crystal Ball. The probability distributions of key parameters are introduced in Section S8 in the Supporting Information. A novel statistical method was developed in this study to evaluate the overall uncertainty of the total Hg emission estimate by model 3, taking into consideration the uncertainty of the relationship between inlet Hg concentration and Hg removal efficiency of APCDs. The slope of the linear relationship in Figure 1 is normally distributed, and the standard deviation of the slope was obtained statistically.[38] The normal distribution of the slope was incorporated into the Monte Carlo simulation. Details of this method can be found in Section S8 in the Supporting Information. The number of sampling was set to be 100,000. When the statistical distribution of Hg emission was obtained, the median value (P50) was considered as the best estimate, and the overall uncertainty of the emission was estimated based on a novel method developed in our previous study,[9] which can be described by the following equation

$$u^{\pm} = \frac{\mathrm{Mo} - \sqrt{\sigma_s^{\pm}\sigma_k^{\pm}}}{\mathrm{P50}} - 1 \quad (4)$$

where u is the uncertainty; Mo is the mode value; σ_s^- and σ_s^+ are the distances between Mo and the values where the probability is equal to $f(\mathrm{Mo})/2$; σ_k^- and σ_k^+ are the distances between Mo and P20 or P80.

The sensitivity analysis function in Crystal Ball was used to quantify the contribution of the uncertainties in input parameters to the overall uncertainty.

3. RESULTS AND DISCUSSION

3.1. Impact of the Removal Compensation Effect on Hg Removal across APCDs. Before introducing the results of Hg emission inventories from the three models, here we present the comparison of probability distributions of the Hg removal efficiencies between model 2 and model 3 to better illustrate the impact of the Hg removal compensation effect. The case of the combination of (FGS + ESD) + DCDA was utilized as an example. Figure 2 demonstrates the impact of the Hg removal compensation effect on the probability distribution of the overall Hg removal efficiency of cascaded APCDs. In model 2, the Hg removal efficiencies of FGS + ESD and DCDA were both assumed to fit normal distribution and were independent of each other, the same as the assumptions in previous studies[19,20] using probabilistic models. The probability distribution of the overall Hg removal efficiency of (FGS + ESD) + DCDA turned out to be negatively skewed with a median value of 97.4%.

In model 3, the Hg removal efficiency of FGS + ESD was divided into two types with high- and low-efficiency scrubbers. The one with the high-efficiency scrubber had more concentrated probability distribution. With the consideration of the relationship between the inlet total Hg concentration in flue gas and the Hg removal efficiency of DCDA, the highly skewed distribution (lognormal) of the Hg content of the

https://doi.org/10.1021/acs.est.1c05523
Environ. Sci. Technol. 2022, 56, 2163−2171

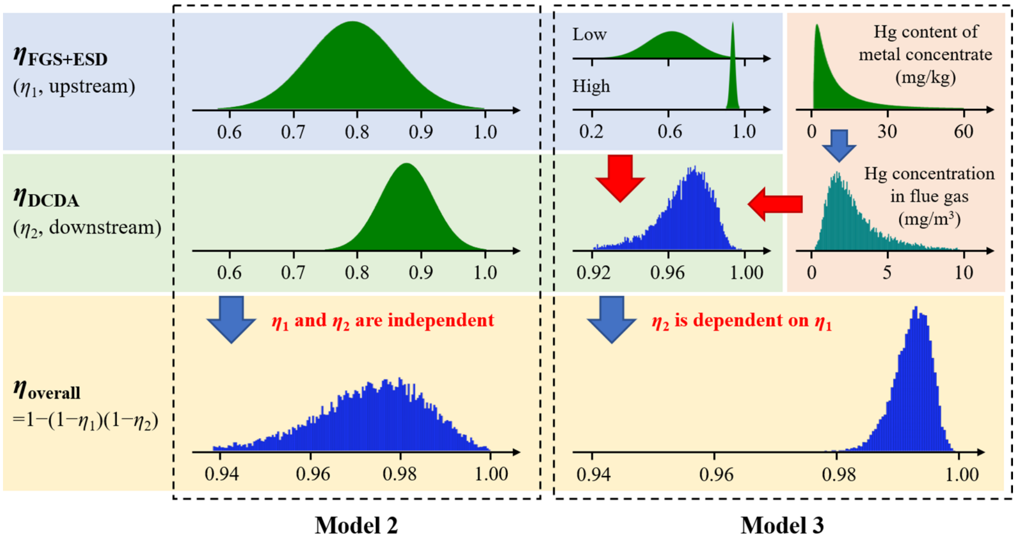

Figure 2. Impact of the Hg removal compensation effect on the probability distribution of the overall Hg removal efficiency of cascaded APCDs (FGS + ESD + DCDA). Note that model 2 is the probabilistic mass flow model, and model 3 is the advanced probabilistic mass flow model taking the Hg removal compensation effect into consideration.

metal concentrate (by province) was passed onto the Hg concentration in flue gas via the Monte Carlo simulation and further onto the Hg removal efficiency of DCDA, resulting in a negatively skewed distribution. In terms of the Hg removal compensation effect, the efficiency of the downstream DCDA was dependent on the efficiency of the upstream FGS + ESD. Consequently, the probability distribution of the overall Hg removal efficiency of (FGS + ESD) + DCDA in model 3 was negatively skewed as well and much more concentrated than in model 2. Due to the difference in the Hg content of Zn, Pb, and Cu concentrates, the probability distributions of the Hg removal efficiencies of (FGS + ESD) + DCDA for the smelting of the three metals were also different (as shown in Figure S4). The high Hg contents of Zn and Pb concentrates led to high overall Hg removal efficiencies of (FGS + ESD) + DCDA for Zn and Pb smelting (mostly above 99%).

3.2. Impact of the Removal Compensation Effect on Hg Emission Inventories for NFMS.

3.2.1. Atmospheric Hg Emission Inventories and Effectiveness of APCDs for NFMS. The atmospheric Hg emissions from NFMS in China in 2010 and 2017 based on the three models are shown in Figure 3. With the deterministic mass flow model (model 1), the atmospheric Hg emissions of the NFMS in 2010 and 2017 were estimated to be 63.5 and 31.4 t, respectively. Since the Hg contents in the metal concentrates used were geometric means, the estimated emissions from model 1 were significantly lower than the results from model 2. In 2010 and 2017, the best estimates from model 2 were 10.1 t and 16.7 t higher than those from model 3, respectively, as a result of the Hg removal compensation effect. The larger difference between the two models in 2017 was due to the increase of the application rate of DCDA from 2010 to 2017 (as shown in Table S5). It should be noted that the Hg emission from Pb smelting in 2010 estimated by model 3 (28.4 t) was higher than that by model 2 (27.9 t). This was due to the limited applications of high-efficiency FGS and DCDA in Pb smelting. The provincial distribution of Hg emissions from NFMS in China is shown in Figure S5. Hg emissions from this sector were concentrated in the Northwest, Central, and Southwest regions in both 2010

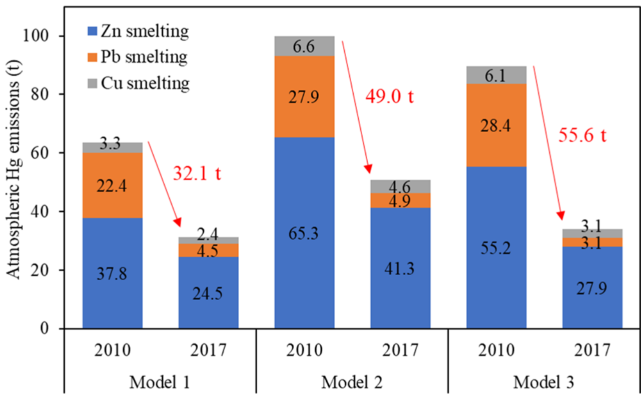

Figure 3. Atmospheric Hg emissions from NFMS estimated by the three models for 2010 and 2017. Note that for the imperial smelting process technology which produces both Zn and Pb, its Hg emission was only considered in Zn smelting. Note that model 1 is the deterministic mass flow model, model 2 is the probabilistic mass flow model, and model 3 is the advanced probabilistic mass flow model taking the Hg removal compensation effect into consideration.

and 2017. The largest difference of Hg emissions between model 2 and model 3 occurred in Gansu and Shaanxi.

The total amounts of Hg emission reduction from 2010 to 2017 estimated by model 1, model 2, and model 3 were 32.1, 49.0, and 55.6 t, respectively. From model 1 to model 2, the effectiveness of APCDs on Hg emission reduction increased because of the rise of total Hg emission estimates. From model 2 to model 3, the effectiveness of APCDs was further boosted due to the consideration of the Hg removal compensation effect. As shown in Figure S5, the effectiveness of APCDs on Hg removal from 2010 to 2017 also exhibited the most enhancement from model 2 to model 3 in Gansu and Shaanxi. It was because the Hg contents of zinc concentrates in these two provinces were much higher than those in the other provinces (as shown in Table S6). Therefore, with the removal compensation effect considered in model 3, a higher Hg concentration in flue gas could lead to a higher overall Hg removal efficiency of APCDs and consequently amplify the effectiveness of control measures.

https://doi.org/10.1021/acs.est.1c05523
Environ. Sci. Technol. 2022, 56, 2163−2171

The best estimates of the total Hg emissions from NFMS in China in 2010 based on model 2 and model 3 were 99.8 and 89.7 t, respectively. The result from model 2 was close to the estimate by Zhang et al.[9] (97.4 t for 2010), while the results from both models were higher than the estimate by Wu et al.[18] (72.5 t for 2010). The lower estimate reported by Wu et al.[18] was due to the application of the geometric means of Hg contents of metal concentrates, just like model 1 in this study. The best estimates for 2017 based on model 2 and model 3 were 50.8 and 34.1 t, respectively, which were significantly lower than the estimate by Liu et al.[10] (68 t for 2017). This was related to the difference in the application rates of outdated APCDs in Pb smelting. In the study of Liu et al.,[10] the Pb smelters without DCDA or more advanced APCDs accounted for 20% of the total production capacity. Based on the Notice on Further Strengthening the Elimination of Outdated Production Capacity, such high rates were unreasonable since outdated production capacity was required to eliminate. The application rates of APCDs by smelting technology were updated in this study based on expert consultation.

3.2.2. Atmospheric Hg Emissions by Smelting Technology. The atmospheric Hg emissions from NFMS by smelting technology are shown in Figures S6−S8. From 2010 to 2017, outdated smelting technologies such as the artisanal zinc smelting process and the electric zinc furnace were gradually eliminated, which was the main reason for the Hg emission reduction in Zn smelting and the change of distribution of Hg emissions by smelting technology during this period. Due to the increase in the activity levels, the proportion of Hg emission from the advanced electrolytic process (EP) technology has increased significantly from 51.2% in 2010 to 89.5% in 2017 (based on model 3), as shown in Figure S6. The difference between the two models was relatively small because the application rates of DCDA were high for all the dominant smelting processes in 2010 and 2017, resulting in the Hg emissions from most smelting processes dropping by an equivalent percentage for the same year from model 2 to model 3.

Similar results were obtained for Pb and Cu smelting, as shown in Figures S7 and S8. The difference in the proportions of Hg emissions by smelting technology between the two inventory years was significant, while the discrepancy between the two models was relatively small. The more advanced smelting technologies such as the rich-oxygen pool smelting process and the flash furnace smelting process contributed more to the total Hg emission from 2010 to 2017 for Pb and Cu smelting, respectively. The share of Hg emission in 2010 from the imperial furnace smelting process technology for Cu smelting, which does not require DCDA, had the largest variation from model 2 (46.3%) to model 3 (50.2%). The increase of the proportion in Hg emission was induced by the Hg removal compensation effect brought by DCDA applications for other smelting technologies.

3.2.3. Atmospheric Hg Emissions at Different Flue Gas Outlets. For the most important smelting technology, the EP technology for Zn smelting, the proportions of Hg emissions from different flue gas outlets have drawn our attention. As shown in Figure 4, Hg emission through the refining flue gas was the leading path for the EP technology. Although acting as the mainstream flue gas, the roasting/smelting flue gas has advanced APCDs with a very high Hg removal efficiency. On the contrary, at the refining stage, the flue gas out of the volatilization kiln only passes through the dust remover and FGD with limited Hg removal efficiency. Based on model 2, the Hg emission proportions of different flue gases almost remained the same from 2010 to 2017. However, according to the results from model 3, the contribution of the refining flue gas increased from 70.7% (2010) to 82.8% (2017), while that of the roasting/smelting flue gas decreased from 21.3 to 5.4% during this period. It can be inferred from the comparison that the effectiveness of advanced APCDs (e.g., DCDA) on Hg removal from the mainstream flue gas could be underestimated if the removal compensation effect was not considered. Therefore, with the Hg emission reduction potential of the roasting/smelting flue gas reaching a limit, we should pay more attention to the control of Hg emission through the refining flue gas in future.

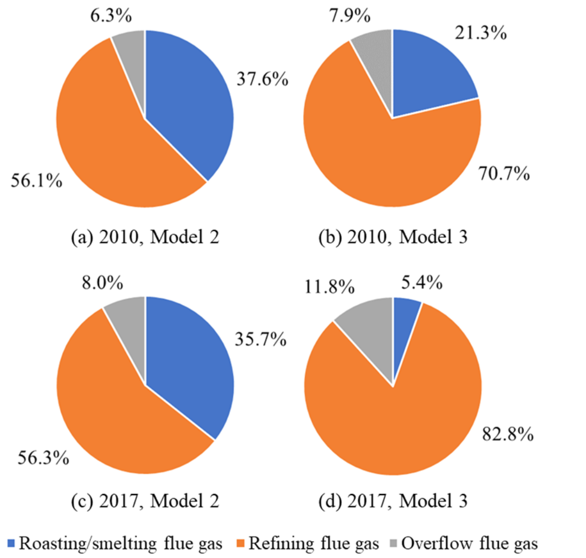

Figure 4. Proportions of Hg emissions from different flue gas outlets in Zn smelters using the EP technology: (a) 2010 model 2, (b) 2010 model 3, (c) 2017 model 2, and (d) 2017 model 3. Note that model 2 is the probabilistic mass flow model, and model 3 is the advanced probabilistic mass flow model taking the Hg removal compensation effect into consideration.

3.3. Impact of the Removal Compensation Effect on Cross-Media Hg Transfer. Figure 5 shows the destinations of Hg in Zn smelting in China. As more FGDs were equipped from 2010 to 2017, more Hg in flue gas was removed and transferred to solid waste, and the proportion of Hg emitted to the atmosphere decreased. According to model 3, due to the increase in the application rate of FGDs in 2017, a higher proportion (22.8%) of Hg was transferred to the solid waste compared to 2010 (16.0%). The differences in Hg destinations between model 2 and model 3 mainly occurred in waste acid and sulfuric acid. Using model 3 with the Hg removal compensation effect considered, the proportion of Hg ended up in sulfuric acid increased significantly compared to model 2, while the proportion entering waste acid decreased. The consideration of removal compensation effect has provided a more accurate approach to investigate the cross-media Hg transfer of NFMS.

The destinations of Hg in Pb and Cu smelting in China are shown in Figures S9 and S10. The variations of Hg transfer destinations in Pb and Cu smelting from 2010 to 2017, especially Pb smelting, were much more significant than in Zn smelting. With the aggressive elimination of outdated smelting

https://doi.org/10.1021/acs.est.1c05523
Environ. Sci. Technol. 2022, 56, 2163−2171

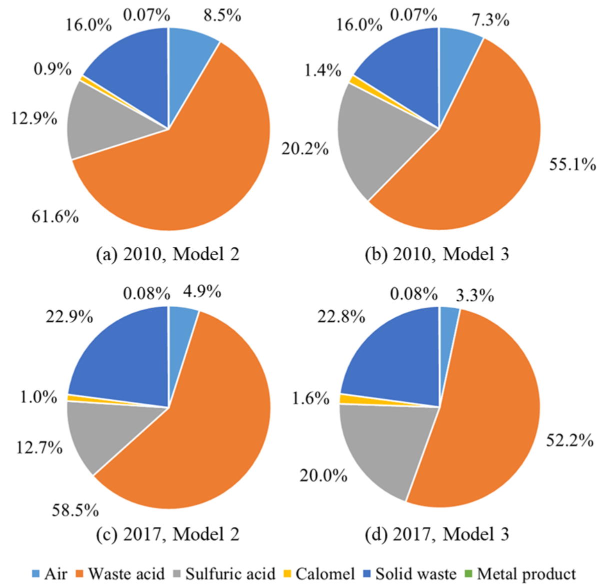

Figure 5. Destinations of Hg in Zn smelting in China: (a) 2010 model 2, (b) 2010 model 3, (c) 2017 model 2, and (d) 2017 model 3. Note that model 2 is the probabilistic mass flow model, and model 3 is the advanced probabilistic mass flow model taking the Hg removal compensation effect into consideration.

technologies and application of high-efficiency APCDs (e.g., FGS + ESD and DCDA) in Pb smelting, a large proportion of Hg in flue gas was transferred to waste acid and sulfuric acid from 2010 to 2017. The differences between model 2 and model 3 for Pb and Cu smelting were similar to Zn smelting. A higher proportion of Hg was transferred to sulfuric acid and a lower proportion of Hg to waste acid in model 3 compared to model 2. The application rate of FGD was still low in Pb smelting and the FGS + ESD + DCDA used in Cu smelting had high Hg removal efficiency, and hence, solid waste was not a major destination of Hg in Pb and Cu smelting.

3.4. Uncertainty Analysis. The uncertainties of atmospheric Hg emissions for the NFMS sector in China based on model 2 and model 3 were evaluated, as shown in Figure S11. In 2010, the uncertainty ranges for Zn, Pb, and Cu smelting and the overall NFMS sector were (−36%, +37%), (−35%, +35%), (−41%, +45%), and (−27%, +27%), respectively, in model 2, and (−34%, +38%), (−33%, +37%), (−39%, +42%), and (−26%, +27%), respectively, in model 3. In our previous study,[9] the uncertainty ranges for the 2010 Hg emission inventories for Zn, Pb, and Cu smelting were (−59%, +72%), (−65%, +84%), and (−59%, +72%), respectively, based on the same uncertainty evaluation methodology. The comparison indicates that the mass flow model yielded lower overall uncertainty than the emission factor model because Hg emissions through different flue gases in the NFMS sector were evaluated separately. However, consideration of the Hg removal compensation effect in model 3 for the 2010 inventories did not show much improvement in uncertainty reduction compared to model 2. This was because Hg emission from the refining flue gas was the main contributor to the total Hg emission, while the Hg removal compensation effect mainly occurred upon the combination of FGS + ESD + DCDA for the mainstream roasting/smelting flue gas.

However, the uncertainties for the 2017 inventories were lower in model 3 than in model 2. The uncertainty ranges for Zn, Pb, and Cu smelting and the overall NFMS sector were (−37%, +39%), (−38%, +40%), (−46%, +49%), and (−31%, +33%), respectively, in model 2 and (−33%, +36%), (−33%, +35%), (−30%, +33%), and (−31%, +31%), respectively, in model 3. The change from 2010 to 2017 was induced by the application of FGDs in both the mainstream roasting/smelting flue gas and the refining flue gas. Therefore, the advantage of the novel methodology of model 3 in uncertainty reduction was revealed in the 2017 case. The uncertainty level of model 3 for 2017 is close to that of the tier 4 method in the CAME model[9] for CFPPs (−35%, +45%).

Based on sensitivity analysis, the uncertainties in model 2 and model 3 were estimated to be mainly attributed to the uncertainties in the Hg contents of metal concentrates for the highly skewed probability distribution. The uncertainties in the Hg removal efficiencies of APCDs also had considerable contribution to the overall uncertainty, although the contribution in model 3 was lower than in model 2. In model 3, the uncertainty of the Hg removal efficiency of FGS + ESD + DCDA was linked to the Hg contents of metal concentrates through a linear relationship and hence greatly reduced (see Figure S4). The contribution from the uncertainty of the linear relationship between Inlet Hg concentration in flue gas and Hg removal efficiency of APCD was not as significant as the contribution from the uncertainty of the Hg contents of metal concentrates.

4. IMPLICATIONS AND LIMITATIONS

To more accurately evaluate the effectiveness of Hg emission control measures for the NFMS sector in China, an improved emission inventory model considering the Hg removal compensation effect was developed in this study. The methodology was crucial for the implementation of the Minamata Convention on Mercury. APCDs applied for the NFMS sector have high Hg removal efficiencies. However, the overall Hg removal efficiency could still be underestimated if the removal compensation effect was neglected. Comparison between model 2 and model 3 showed that the overlook of the effect resulted in an overestimation of Hg emission by 10.1 t in 2010 and 16.7 t in 2017. The impacts on early years were small, while the influence on recently years became more and more significant since more and more advanced APCDs were being put into practice. The total amount of Hg emission reduction in the NFMS sector from 2010 to 2017 was 49.0 t in model 2 and 55.6 t in model 3, resulting in a 13.5% increase, which could affect the effectiveness evaluation of convention implementation.

The Hg removal compensation effect is not a unique phenomenon for the NFMS sector in China, but whether it causes underestimation of Hg removal effectiveness depends on the probability distribution of the Hg content of fuels or raw materials (as illustrated in Figure 2). The methodology developed in this study could be adapted to other key emission sectors such as cement plants. The application of the relationship between inlet Hg concentration in flue gas and the Hg removal efficiency of APCD to the model and the methodology developed in this study to consider the uncertainty of the relationship in the Monte Carlo simulation have reduced both the theoretical bias and the overall uncertainty of the Hg emission estimate. A much lower uncertainty level was found for model 3 compared to the existing studies.[9,10,19]

With the phasing out of outdated smelting technologies, advanced technologies contribute more and more Hg

https://doi.org/10.1021/acs.est.1c05523
Environ. Sci. Technol. 2022, 56, 2163−2171

emissions, which were easier to be abated. However, more efforts were made to the mainstream flue gas, making other flue gases (e.g., the refining flue gas) become the dominant contributors. More attention should be paid to the control of Hg emissions from the flue gas from the refining stage (e.g., the volatilization kiln) in the future. Some provinces in the Northwest use metal concentrates with high Hg contents. Our advanced model suggests that these provinces might have a lower Hg emission level than previously estimated, but Hg reclamation in Zn smelting using metal concentrates from these provinces is still in urgent need. In addition, a large amount of Hg is transferred to waste acid, and the amount of Hg entering sulfuric acid could be underestimated. Strengthening the disposal of waste acid and recovering Hg from sulfuric acid produced by NFMS are of significant importance.

The limitation of this study mainly lies in the relationship between the inlet Hg concentration in flue gas and the Hg removal efficiencies of APCDs. The relationship for wet FGD (WFGD) was adapted from the tests in CFPPs, which could be quite different from the case in smelters. More field measurements should be carried out to further explore the relationship in future studies. Moreover, the Hg removal efficiency of dry FGD (DFGD) was assumed to be zero, which was inherited from previous studies[10,19] based on very limited test results. With the gradual popularization of DFGD and WFGD, more tests are required for FGDs in nonferrous metal smelters.

■ ASSOCIATED CONTENT

Supporting Information

The Supporting Information is available free of charge at https://pubs.acs.org/doi/10.1021/acs.est.1c05523.

Description of the mass flow models and parameters for the models; methodology for uncertainty analysis; and results from the models (PDF)

■ AUTHOR INFORMATION

Corresponding Author

Lei Zhang − *School of the Environment, and State Key Laboratory of Pollution Control and Resource Reuse, Nanjing University, Nanjing, Jiangsu 210023, China; Jiangsu Collaborative Innovation Center of Atmospheric Environment and Equipment Technology (CICAEET), Nanjing University of Information Science and Technology, Nanjing, Jiangsu 210044, China;* orcid.org/0000-0003-2796-6043; Email: lzhang12@nju.edu.cn

Authors

Shuzhen Cao − *School of the Environment, and State Key Laboratory of Pollution Control and Resource Reuse, Nanjing University, Nanjing, Jiangsu 210023, China*

Yang Zhang − *School of the Environment, and State Key Laboratory of Pollution Control and Resource Reuse, Nanjing University, Nanjing, Jiangsu 210023, China*

Shuxiao Wang − *School of Environment, and State Key Joint Laboratory of Environment Simulation and Pollution Control, Tsinghua University, Beijing 100084, China;* orcid.org/0000-0001-9727-1963

Qingru Wu − *School of Environment, and State Key Joint Laboratory of Environment Simulation and Pollution Control, Tsinghua University, Beijing 100084, China;* orcid.org/0000-0003-3381-4767

Complete contact information is available at: https://pubs.acs.org/10.1021/acs.est.1c05523

Notes

The authors declare no competing financial interest.

■ ACKNOWLEDGMENTS

This work was funded by the National Natural Science Foundation of China (no. 21876077) and the Natural Resources Defense Council (NRDC). We thank Zhuqiang Shao and Fengzhou Yue for providing information on the NFMS industry in China and their valuable consultation. We also thank Zhe Wang for her help on the visualization of the results from this study.

■ REFERENCES

(1) Streets, D. G.; Devane, M. K.; Lu, Z.; Bond, T. C.; Sunderland, E. M.; Jacob, D. J. All-time releases of mercury to the atmosphere from human activities. *Environ. Sci. Technol.* **2011**, *45*, 10485−10491.

(2) Obrist, D.; Kirk, J. L.; Zhang, L.; Sunderland, E. M.; Jiskra, M.; Selin, N. E. A review of global environmental mercury processes in response to human and natural perturbations: Changes of emissions, climate, and land use. *Ambio* **2018**, *47*, 116−140.

(3) United Nations Environment Programme (UNEP). *Global Mercury Assessment 2013: Sources, Emissions, Releases and Environmental Transport*; UNEP Chemicals Branch: Geneva, Switzerland, 2013.

(4) Streets, D.; Hao, J.; Wu, Y.; Jiang, J.; Chan, M.; Tian, H.; Feng, X. Anthropogenic mercury emissions in China. *Atmos. Environ.* **2005**, *39*, 7789−7806.

(5) Pirrone, N.; Cinnirella, S.; Feng, X.; Finkelman, R. B.; Friedli, H. R.; Leaner, J.; Mason, R.; Mukherjee, A. B.; Stracher, G. B.; Streets, D. G.; Telmer, K. Global mercury emissions to the atmosphere from anthropogenic and natural sources. *Atmos. Chem. Phys.* **2010**, *10*, 5951−5964.

(6) Pacyna, E. G.; Pacyna, J. M.; Sundseth, K.; Munthe, J.; Kindbom, K.; Wilson, S.; Steenhuisen, F.; Maxson, P. Global emission of mercury to the atmosphere from anthropogenic sources in 2005 and projections to 2020. *Atmos. Environ.* **2010**, *44*, 2487−2499.

(7) Zhu, C.; Tian, H.; Hao, J. Global anthropogenic atmospheric emission inventory of twelve typical hazardous trace elements. *Atmos. Environ.* **2020**, *220*, 1995−2012.

(8) Selin, H.; Keane, S. E.; Wang, S.; Selin, N. E.; Davis, K.; Bally, D. Linking science and policy to support the implementation of the Minamata Convention on Mercury. *Ambio* **2018**, *47*, 198−215.

(9) Zhang, L.; Wang, S.; Wang, L.; Wu, Y.; Duan, L.; Wu, Q.; Wang, F.; Yang, M.; Yang, H.; Hao, J.; Liu, X. Updated emission inventories for speciated atmospheric mercury from anthropogenic sources in China. *Environ. Sci. Technol.* **2015**, *49*, 3185−3194.

(10) Liu, K.; Wu, Q.; Wang, L.; Wang, S.; Liu, T.; Ding, D.; Tang, Y.; Li, G.; Tian, H.; Duan, L.; Wang, X.; Fu, X.; Feng, X.; Hao, J. Measure-specific effectiveness of air pollution control on China's atmospheric mercury concentration and deposition during 2013-2017. *Environ. Sci. Technol.* **2019**, *53*, 8938−8946.

(11) Pacyna, E.; Pacyna, J. Global emission of mercury from anthropogenic sources in 1995. *Water Air Soil Pollut.* **2002**, *137*, 149−165.

(12) Pacyna, E. G.; Pacyna, J. M.; Steenhuisen, F.; Wilson, S. Global anthropogenic mercury emission inventory for 2000. *Atmos. Environ.* **2006**, *40*, 4048−4063.

(13) United Nations Economic Commission for Europe (UNECE). *Joint EMEP/CORINAIR Atmospheric Emission Inventory Guidebook*; UNECE: Geneva, Switzerland, 2000.

(14) Wu, Y.; Wang, S.; Streets, D. G.; Hao, J.; Chan, M.; Jiang, J. Trends in anthropogenic mercury emissions in China from 1995 to 2003. *Environ. Sci. Technol.* **2006**, *40*, 5312−5318.

(15) Jiang, J. *Preliminary Studies on Emission and Control of Atmosphere Mercury in China*. Masters Dissertation, Tsinghua University, Beijing, China, 2004.
(16) Feng, X.; Li, G.; Qiu, G. A preliminary study on mercury contamination to the environment from artisanal zinc smelting using indigenous methods in Hezhang county, Guizhou, China—Part 1: mercury emission from zinc smelting and its influences on the surface waters. *Atmos. Environ.* **2004**, *38*, 6223−6230.
(17) Hylander, L. D.; Herbert, R. B. Global emission and production of mercury during the pyrometallurgical extraction of nonferrous sulfide ores. *Environ. Sci. Technol.* **2008**, *42*, 5971−5977.
(18) Wu, Q. R.; Wang, S. X.; Zhang, L.; Song, J. X.; Yang, H.; Meng, Y. Update of mercury emissions from China's primary zinc, lead and copper smelters, 2000-2010. *Atmos. Chem. Phys.* **2012**, *12*, 11153−11163.
(19) Wu, Q.; Wang, S.; Li, G.; Liang, S.; Lin, C.-J.; Wang, Y.; Cai, S.; Liu, K.; Hao, J. Temporal trend and spatial distribution of speciated atmospheric mercury emissions in China during 1978-2014. *Environ. Sci. Technol.* **2016**, *50*, 13428−13435.
(20) Wu, Q.; Wang, S.; Zhang, L.; Hui, M.; Wang, F.; Hao, J. Flow analysis of the mercury associated with nonferrous ore concentrates: Implications on mercury emissions and recovery in China. *Environ. Sci. Technol.* **2016**, *50*, 1796−1803.
(21) Song, J. X.; Wang, S. X.; Li, G. H. Spatial distribution of mercury content of zinc concentrates in China. *Science* **2010**, *5*, 472−475.
(22) Wang, S. X.; Song, J. X.; Li, G. H.; Wu, Y.; Zhang, L.; Wan, Q.; Streets, D. G.; Chin, C. K.; Hao, J. M. Estimating mercury emissions from a zinc smelter in relation to China's mercury control policies. *Environ. Pollut.* **2010**, *158*, 3347−3353.
(23) Zhang, L.; Wang, S.; Wu, Q.; Meng, Y.; Yang, H.; Wang, F.; Hao, J. Were mercury emission factors for Chinese non-ferrous metal smelters overestimated? Evidence from onsite measurements in six smelters. *Environ. Pollut.* **2012**, *171*, 109−117.
(24) Wu, Q. R. Characteristics and abatement potential of mercury emission for China's nonferrous metal smelting industries. Ph.D. Thesis, Tsinghua University, Beijing, China, 2015.
(25) Hui, M.; Wu, Q.; Wang, S.; Liang, S.; Zhang, L.; Wang, F.; Lenzen, M.; Wang, Y.; Xu, L.; Lin, Z.; Yang, H.; Lin, Y.; Larssen, T.; Xu, M.; Hao, J. Mercury flows in China and global drivers. *Environ. Sci. Technol.* **2017**, *51*, 222−231.
(26) Wu, Q.; Wang, S.; Wang, Z.; Li, K. Study on mercury emission characteristics during leaching slags disposal process in the rotary kilns of Zn smelters. *China Environ. Sci.* **2017**, *37*, 2513−2519.
(27) Wu, Q.; Wang, S.; Hui, M.; Wang, F.; Zhang, L.; Duan, L.; Luo, Y. New insight into atmospheric mercury emissions from zinc smelters using mass flow analysis. *Environ. Sci. Technol.* **2015**, *49*, 3532−3539.
(28) Zhang, L.; Wang, S.; Meng, Y.; Hao, J. Influence of mercury and chlorine content of coal on mercury emissions from coal-fired power plants in China. *Environ. Sci. Technol.* **2012**, *46*, 6385−6392.
(29) Meij, R.; te Winkel, H. Mercury emissions from coal-fired power stations: The current state of the art in the Netherlands. *Sci. Total Environ.* **2006**, *368*, 393−396.
(30) Li, G.; Feng, X.; Li, Z.; Qiu, G.; Shang, L.; Liang, P.; Wang, D.; Yang, Y. Mercury emission to atmosphere from primary Zn production in China. *Sci. Total Environ.* **2010**, *408*, 4607−4612.
(31) Nonferrous Metal Industry Association of China (NMIA). *Yearbook of Nonferrous Metals Industry of China*; NMIA: Beijing, China, 2011.
(32) Nonferrous Metal Industry Association of China (NMIA). *Yearbook of Nonferrous Metals Industry of China*; NMIA: Beijing, China, 2018.
(33) Wu, Q.; Li, G.; Wang, S.; Liu, K.; Hao, J. Mitigation options of atmospheric Hg emissions in China. *Environ. Sci. Technol.* **2018**, *52*, 12368−12375.
(34) Wu, Q.; Wang, S.; Hui, M.; Wang, F.; Zhang, L.; Duan, L.; Luo, Y. New insight into atmospheric mercury emissions from zinc smelters using mass flow analysis. *Environ. Sci. Technol.* **2015**, *49*, 3532−3539.
(35) Wang, S. X.; Zhang, L.; Li, G. H.; Wu, Y.; Hao, J. M.; Pirrone, N.; Sprovieri, F.; Ancora, M. P. Mercury emission and speciation of coal-fired power plants in China. *Atmos. Chem. Phys.* **2010**, *10*, 1183−1192.
(36) Zhang, L. Emission characteristics and synergistic control strategies of atmospheric mercury from coal combustion in China. Ph.D. Thesis, Tsinghua University, Beijing, China, 2012.
(37) Zhang, L.; Daukoru, M.; Torkamani, S.; Wang, S.; Hao, J.; Biswas, P. Measurements of mercury speciation and fine particle size distribution on combustion of China coal seams. *Fuel* **2013**, *104*, 732−738.
(38) Berthouex, P. M.; Brown, L. C. *Statistics for Environmental Engineering*; Lewis Publishers: Boca Raton, Florida, USA, 2002.

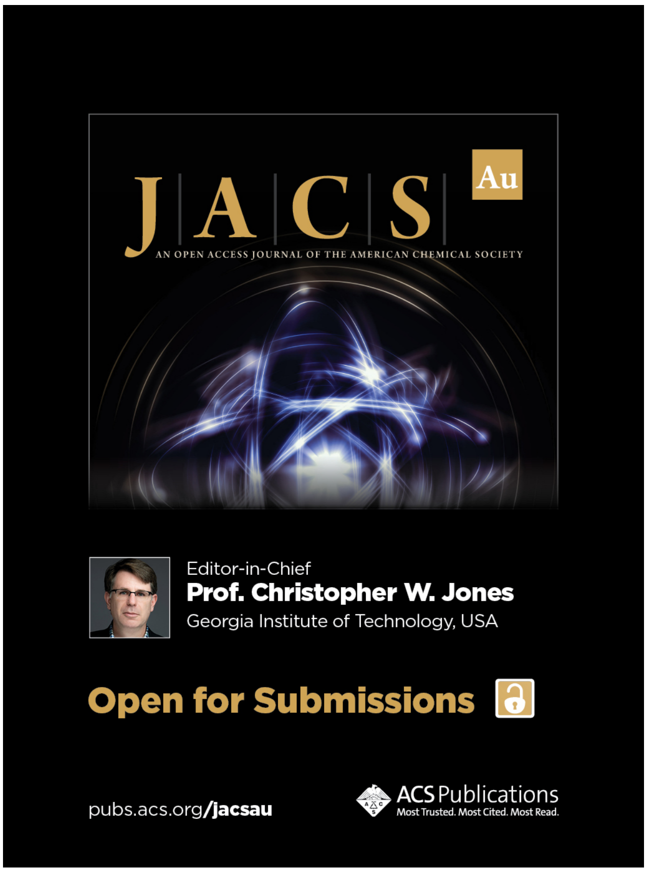

https://doi.org/10.1021/acs.est.1c05523
Environ. Sci. Technol. 2022, 56, 2163−2171